J. Membrane Biol. 87, 159–172 (1985)

The Journal of
Membrane Biology

The Mechanistic Nature of the Membrane Potential Dependence of Sodium-Sugar Cotransport in Small Intestine

Diego Restrepo and George A. Kimmich
Department of Radiation Biology and Biophysics, University of Rochester School of Medicine and Dentistry, Rochester, New York 14642

Summary. Methods are described which demonstrate the use of unidirectional influx of ^{14}C-tetraphenylphosphonium (^{14}C-TPP$^+$) into isolated intestinal epithelial cells as a quantitative sensor of the magnitude of membrane potentials created by experimentally imposed ion gradients. Using this technique the quantitative relationship between membrane potential ($\Delta\psi$) and Na^+-dependent sugar influx was determined for these cells at various Na^+ and α-methylglucoside (α-MG) concentrations. The results show a high degree of $\Delta\psi$ dependence for the transport Michaelis constant but a maximum velocity for transport which is independent of $\Delta\psi$. No transinhibition by intracellular sugar (40 mM) can be detected. Sugar influx in the absence of Na^+ is insensitive to 1.3 mM phlorizin and independent of $\Delta\psi$. The mechanistic implications of these results were evaluated using the quality of fit between calculated and experimentally observed kinetic constants for rate equations derived from several transport models. The analysis shows that for models in which translocation is the potential-dependent step the free carrier cannot be neutral. If it is anionic, the transporter must be functionally asymmetric. A model in which Na^+ binding is the potential-dependent step (Na^+ well concept) also provides an appropriate kinetic fit to the experimental data, and must be considered as a possible mechanistic basis for function of the system.

Key Words cotransport · membrane potential · TPP$^+$ influx technique · sodium-dependent sugar transport · coupling · small intestine · kinetic analysis of sugar transport

Introduction

The rheogenicity of Na^+-dependent sugar and amino-acid transport in small intestine was first demonstrated by White and Armstrong (1971) and Rose and Schultz (1971). Three years later, Murer and Hopfer (1974) showed that Na^+-dependent influx of sugar in small intestine is a function of the membrane potential. Since then, a number of investigators have confirmed this dependence and have widened our knowledge of its nature (Carter-Su & Kimmich, 1979; Kanuitz & Wright, 1984). More recent developments have indicated that the binding of phlorizin, a competitive inhibitor of Na^{2+}-sugar cotransport to brush-border membranes, is enhanced by inside-negative membrane potentials (Tannenbaum et al., 1977; Aronson, 1978; Toggenburger et al., 1978, 1982; Turner & Silverman, 1981) and that transinhibition of the transport system by sugar is relieved by inside-negative potential differences (Kessler & Semenza, 1983). On the basis of the latter findings and kinetic studies of the transporter, Kessler and Semenza have proposed a model which can qualitatively explain the observed membrane potential dependence of Na^+-sugar cotransport (Kessler & Semenza, 1983; Semenza et al., 1984, 1985). However, despite the large amount of qualitative information available on the membrane potential dependence of Na^+-sugar cotransport in small intestine, there is a surprisingly small amount of information about the quantitative details of this dependence.

The lack of quantitative information can be explained by the absence of an adequate technique to measure the membrane potential under the same experimental conditions that sugar fluxes are measured. Recently, Wright and co-workers have used carbocyanine dyes in membrane vesicles to measure the membrane potential (Schell et al., 1983; Gunther et al., 1984). However, these authors have not reported the use of these dyes to investigate the quantitative dependence of sugar influx on the measured potential difference. In the past year, we have been exploring a different approach for measuring the membrane potential which depends on the unidirectional influx of the lipophilic cation tetraphenylphosphonium (TPP$^+$) as a potential sensor. We have already demonstrated the use of TPP$^+$ influx for measuring relative ion permeabilities in isolated chick intestinal epithelial cells (Kimmich et al., 1985*a*). A related approach was used to define the basic features of the potential dependence for the sodium-dependent sugar transport system (Kimmich et al., 1985*b*). As suggested earlier (Kimmich

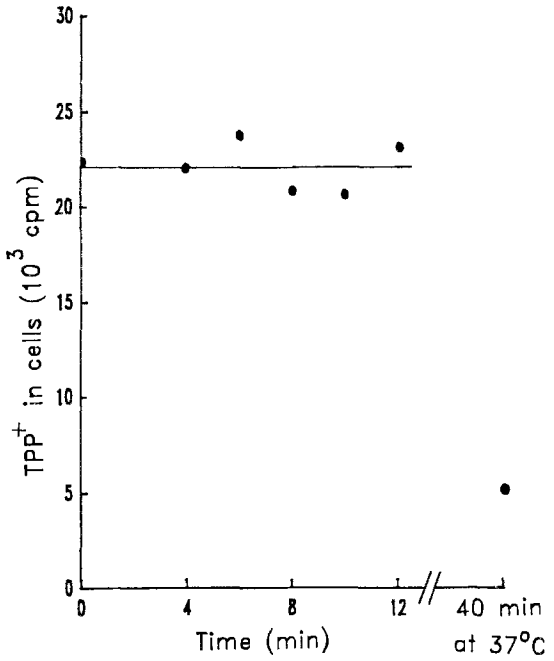

Fig. 1. Retention of [^{14}C]-TPP^+ by cells diluted in cold wash media. Cells were isolated in media containing 140 mM K-gluconate (KG) and were de-energized as described in Materials and Methods in the presence of 30 μg/ml valinomycin. After a 15-min preincubation at 37°C, cells were resuspended and incubated for 20 min with a trace amount of radioactive TPP^+ (1.5 μCi/ml; 31.4 mCi/mmol). The cells were then diluted 80-fold into ice-cold stop media (*see* Materials and Methods). Effluxes were stopped by centrifugation. Two effluxes were carried out at 37°C for 40 min. Results shown are from one experiment

et al., 1985*b*; Restrepo & Kimmich, 1985*b*) and confirmed here, the unidirectional influx of TPP^+ follows the behavior predicted by the Goldman flux equation (Goldman, 1943). Using this relationship as a calibration curve we have used TPP^+ influx to measure membrane potential differences and hence to establish the quantitative electrical potential dependence of Na^+-sugar cotransport.

Materials and Methods

Cell Isolation and ATP Depletion

Chick intestinal cells were isolated by the hyaluronidase digestion procedure reported earlier (Kimmich, 1970). Briefly, a defined portion of the intestine is slit lengthwise and cut into segments 2 to 3 inches in length. The tissue is incubated in a solution containing hyaluronidase (Sigma type I-S), 1 mg/ml, for 35 min at 37°C. After this incubation, villus cells are detached from the tissue by gentle agitation with a plastic pipette. Cells are washed free of the hyaluronidase by centrifugation and resuspension and preincubated in different solutions depending on the particular experiment. ATP depletion is accomplished by incubation with 80 μM rotenone and 200 μM ouabain (Carter-Su & Kimmich, 1979). After isolation, cells are placed on ice and are used within 1 or 2 hr of preparation.

For the experiments in which unidirectional influx of TTP^+ or sugar was measured, the cells typically were isolated in KG medium containing (in mM): 140 K-gluconate, 1 $CaSO_4$, 1 $MgSO_4$, 25 HEPES-Tris[1] (pH 7.4 at 37°C) and 1 mg/ml BSA (bovine serum albumin; Sigma fraction V). This solution had an osmolarity of approximately 300 mosm (measured using a Fiske osmometer). When large amounts of sugar or ions were required by the experimental protocol, cells were isolated in hyperosmolar media (indicated in the respective figure legends). The ionic composition of other media used is: KCl medium, same as KG except all gluconate and sulfate were replaced by chloride; TG medium, same as KG except potassium was replaced by tetramethylammonium (TMA^+); TCl medium which is KG medium with potassium replaced by TMA^+ and gluconate and sulfate replaced by chloride. All chemicals were of the highest purity available.

Radioactive Isotope Uptake

The intracellular content of [^{14}C]-α-methylglucoside (αMG), [^{14}C]-tetraphenylphosphonium (TPP^+) and [^{14}C]-3-O-methylglucose (3-OMG) were determined using a centrifugation procedure to separate cells from incubation medium. Cells and media were warmed to 37°C in separate incubation vessels. At time zero, a small aliquot of cells (50 to 200 μl of 6 to 15% vol/vol cells) was added to 0.8 to 2.0 ml of medium containing the radioactive isotope. Aliquots (50 to 200 μl) were sampled at intervals of 4 to 12 sec and the aliquots diluted into 4 ml of ice-cold stop media (25 mM HEPES-Tris, pH 7.4, 1 mg/ml BSA and enough mannitol to make the wash solution isosmolar with the incubation solution). The diluted aliquots were centrifuged for 10 sec at 8000 $\times$ *g* in an Adams MHCT tabletop centrifuge and washed once with 2 ml of cold stop solution. The entire wash procedure required 3 to 3.5 min. Control experiments have shown that the ice-cold stop prevents subsequent loss of sugar during the wash interval (Picone, 1977). Retention of radioactive TPP^+ inside cells placed in ice-cold stop media is shown in Fig. 1. The washed pellets were dissolved in Liquiscint® (National Diagnostics) and counted in a Beckman LS-230 liquid scintillation counter. The concentration of TPP^+ varied between 6 and 16 μM (0.2 to 0.5 μCi/ml) depending on the particular experimental protocol.

[^{14}C]-Tetraphenylphosphonium was purchased from New England Nuclear. All other radioisotopes were from Amersham.

3-O-Methylglucose Space Determination

Unidirectional influxes of αMG were normalized by dividing the rates in nmol/min by the intracellular 3-OMG space expressed in μl for an equivalent sample of cells. In order to determine intracellular 3-OMG space in a given sample, the amount of [^{14}C]-3-O-methylglucose inside the cells was measured after a steady-state distribution had been attained at 37°C in media containing 480

[1] N-2-hydroxyethylpiperazine-N'-2-ethanesulfonic acid (Sigma Chemical).

μM phlorizin. Typically, a 15-min incubation is long enough to allow complete equilibration of the sugar. The intracellular 3-OMG space was calculated using the measured intracellular 3-OMG content and the volume specific activity (cpm/μl) of the radioactive sugar in the incubation media. In previous studies (Restrepo & Kimmich, 1985*a*) we have normalized fluxes to the amount of cellular protein. For comparative purposes, we determined that in cells isolated in KG media there are 1.73 ± 0.15 μl/mg cellular protein (mean ± SD, n = 9). Protein was measured employing the biuret method (Gornall et al., 1979) using BSA as a standard. The main advantage of measuring 3-OMG volumes is that the procedure is faster than the protein assay.

Intracellular Volume Determination by Double Labeling

Total intracellular volume was determined by double labeling using tritiated water as the intracellular space marker and [^{14}C]-polyethylene glycol ([^{14}C]-PEG, avg mol wt 4000) as extracellular marker. In control experiments it was determined that tritiated water equilibrates in less than 10 sec and that [^{14}C]-PEG does not enter the cells appreciably for incubation periods as long as 30 min (*data not shown*). The standard procedure involves mixing a 50-μl aliquot of cells containing 1.5 to 3.0 mg of cellular protein with 4.0 ml of media containing 2.5 μCi of [^{3}H]-water and 0.1 μCi of [^{14}C]-PEG at 37°C and centrifuging immediately. The pellet and two 25-μl samples of the supernatant were counted and converted to dpm in a Packard Tri-carb 460C scintillation counter using the external standard for quench correction. Identical space values were obtained when longer intervals were allowed before centrifugation.

Sodium and Potassium Determination by Flame Photometry

Intracellular potassium (K_i^+) was determined by measuring the potassium concentration in 3% TCA extracts of cell pellets that had been washed as described above for the radioactive isotope influx experiments. Potassium content was measured with a flame photometer (Instrumentation Laboratories model 143). Lithium was used as internal standard. The intracellular potassium concentration was then calculated using the intracellular volume determined using the double-label intracellular volume technique described above. Sodium concentrations were determined using the same procedure.

Calculation of the Membrane Potential from the TPP^+ Influx

The unidirectional influx of TPP^+ at zero membrane potential was used to normalize all TPP^+ fluxes. For cells isolated in KG media this was accomplished by measuring influx of the lipophilic cation into cells diluted in KG media plus 20 to 40 μg/ml of valinomycin. All influxes at other potentials were divided by the zero potential flux, and the membrane potential was determined using the Goldman flux equation (Eq. 2). This normalization procedure avoids the need to have a value for the permeability of tetraphenylphosphonium which otherwise would have to be obtained by independent methods.

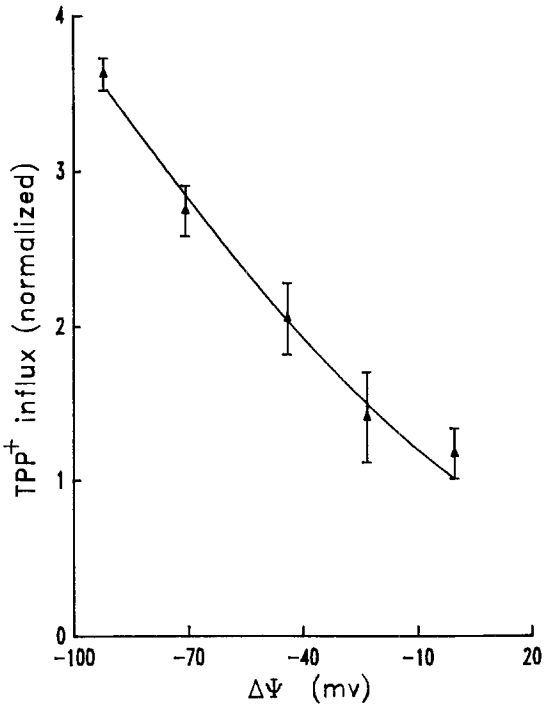

Fig. 2. TPP^+ influx *vs.* calculated membrane potential. Cells were isolated in KG media and de-energized as described in Materials and Methods. 30 μg/ml of valinomycin were added after cell isolation. After a 20-min preincubation at 37°C, the influx of radioactive TPP^+ was monitored in cells with different imposed K^+ gradients. K-gluconate was replaced by TMA-gluconate. (Outside potassium concentrations were 145, 71.4, 35.2, 13.4 and 6.2 mM.) The influx values were calculated using a linear regression on six points taken every 4.8 sec. The membrane potential was calculated as stated in Materials and Methods (*also see* Results). The results shown are the average ± SD from three experiments. The solid line is the least-squares fit of the Goldman flux equation (Eq. 2) to the data

Data Analysis

Nonlinear least-squares fit of the experimental data was accomplished using the maximum neighborhood algorithm reported previously (Restrepo & Kimmich, 1985*a*) and the simplex algorithm (Caceci & Cacheris, 1984).

Results

Using TPP^+ Influx to Measure Membrane Potentials

When ATP-depleted cells isolated in KG media in the presence of valinomycin are transferred to media with different K^+ concentrations, TPP^+ influx increases as extracellular potassium is decreased (*see* Fig. 2). This is to be expected due to the valinomycin-induced enhancement of conductive K^+ per-

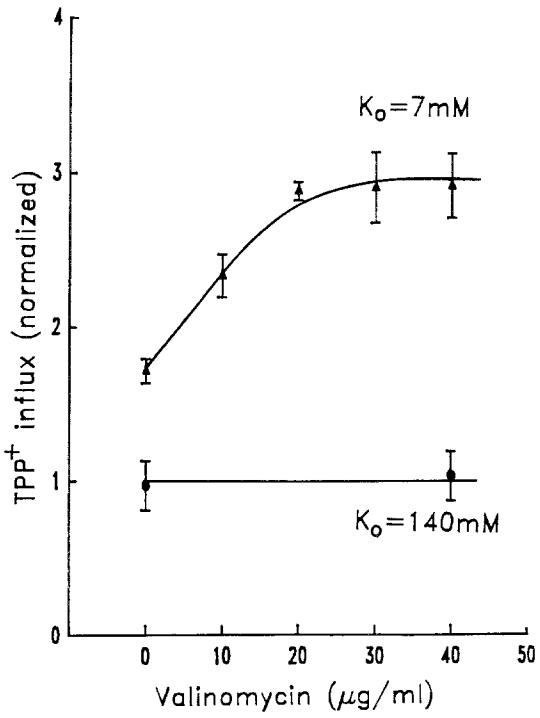

Fig. 3. TPP^+ influx *vs.* valinomycin concentration. Cells were isolated and de-energized in KG media. They were preincubated for 20 min (45 to 60 mg/ml cell protein) in the presence of varying amounts of valinomycin (0 to 40 μg/ml). Influx of TPP^+ was started after a 20-fold dilution into media containing either 140 mM K-gluconate (circles) or 140 mM TMA-gluconate (triangles). Results shown are the average from three experiments ± SD

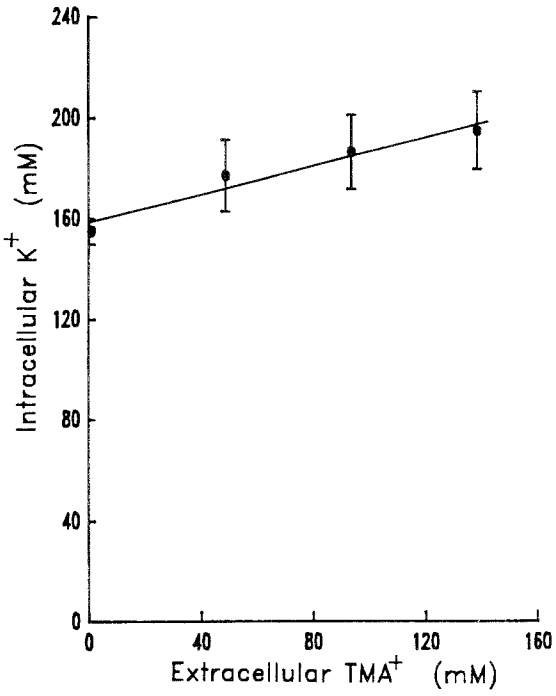

Fig. 4. Intracellular potassium concentration *vs.* TMA^+ concentration of the outside media. Cells were isolated and de-energized in KG media. After a 10-min preincubation with 30 μg/ml valinomycin, cells were assayed for potassium content and for intracellular volume (*see* Materials and Methods). Volumes were measured for cells diluted into media with K-gluconate replaced by varying amounts of TMA-gluconate. The results shown are the average ± SD for four determinations at each TMA^+ concentration in one experiment

meability and the consequent inside-negative diffusion potentials. Figure 2 shows the experimentally determined dependence of TPP^+ influx on membrane potential. The membrane potentials indicated were calculated using the Nernst equation.

$$\Delta\psi = (RT/F)\ \ln(K_o/K_i). \quad (1)$$

The calculated potentials are accurate provided that the permeability of potassium is much larger than that of all other ions present in the system and that the intracellular potassium concentration is determined accurately. We have performed control experiments to evaluate these two assumptions as discussed below.

Valinomycin is commonly used to specifically increase the electrogenic potassium permeability relative to that of other ions. However, as we have pointed out earlier, potentials calculated by the Nernst equation are within 5% of the true value of the membrane potential only when the permeability for potassium is 200- to 400-fold greater than the permeability of other ions in the system (Kimmich et al., 1985*b*). In order to test whether the concentration of valinomycin is large enough to increase the potassium permeability by the required amount, we performed experiments in which TPP^+ influx was used as a qualitative sensor of the membrane potential. Figure 3 shows that, as expected, if a potassium gradient is present ($K_o < K_i$), TPP^+ influx increases as valinomycin concentration is increased at low concentrations. At valinomycin concentrations greater than 20 μg/ml, TPP^+ influx (i.e. the membrane potential) does not change as the valinomycin concentration is raised further. This indicates that at concentrations of valinomycin larger than 20 μg/ml the membrane potential is close to the K^+ equilibrium potential for the conditions of this experiment. The plateau in the membrane potential is not a nonspecific effect of valinomycin on TPP^+ influx since, in the absence of a potassium gradient, TPP^+ influx does not change upon addition of the largest concentration of valinomycin used.

For ATP-depleted cells isolated in KG media (145 ± 7.5 mM potassium, avg ± SD, n = 6) the average intracellular potassium concentration is 480

± 120 nmol of K^+ per mg of cellular protein (avg ± SD, n = 6). This yields an intracellular potassium concentration of 147 ± 21 mM (avg ± SD, n = 6) when the intracellular volume of cells in KG media is measured using the double-label technique (3.25 ± 0.53 μl/mg, avg ± SD, n = 6). However, when cells are diluted 80-fold into a medium containing 140 mM TMA-gluconate instead of K-gluconate, the measured volume is 2.45 ± 0.44 μl/mg (avg ± SD, n = 6). This volume change is complete within less than 10 sec and is stable up to 20 min (*data not shown*). Since the half-time for K^+ efflux under these conditions is approximately 8 min, the rapid volume change leads to a sudden change in intracellular potassium concentration which must be taken into account when calculating the K^+ equilibrium potentials for the experiments in Fig. 2. The change in intracellular potassium concentration as a function of outside TMA^+ concentration is shown in Fig. 4.

In order to correct for the changes in intracellular potassium concentration, the membrane potentials shown in Fig. 2 were calculated assuming that the intracellular potassium concentration follows a straight line relationship as a function of extracellular TMA^+ as shown in Fig. 4. For this purpose, intracellular potassium and volume determinations established in six experiments under the conditions of the experiments of Fig. 2 (*see* Materials and Methods) were employed. If the volume change is not considered and if it is assumed that intracellular potassium is equal to the extracellular potassium concentration of the preincubation medium, the largest error in the calculated potential would have been 8 mV for the point at −92.2 mV (9%). Hence, we have established that errors in the calculated potentials are small (less than 9%), and we have corrected the potentials in Fig. 2 for these small errors.

The results shown in Figs. 3 and 4 allow us to use the Nernst equation with the appropriate potassium concentrations to calculate the membrane potential for the experiments shown in Fig. 2. The data in this figure are fit by the Goldman flux equation (Goldman, 1943).

$$J = -PCx/(1 - e^x) \qquad (2)$$

where $x = \Delta\psi F/RT$. This relationship can be used to determine unknown potentials by expressing the rate of TPP^+ influx at the unknown potential as a multiple of the rate of TPP^+ influx at zero potential and using Fig. 2 as a calibration relationship for calculating the unknown potential. Note that the fluxes in Fig. 2 are all given relative to the flux at zero potential which is arbitrarily assigned the value of 1. This procedure is used in subsequent figures where the dependence of Na^+-dependent sugar fluxes on $\Delta\psi$ is investigated quantitatively. It circumvents the necessity of having a separately determined value for the permeability constant of TPP^+.

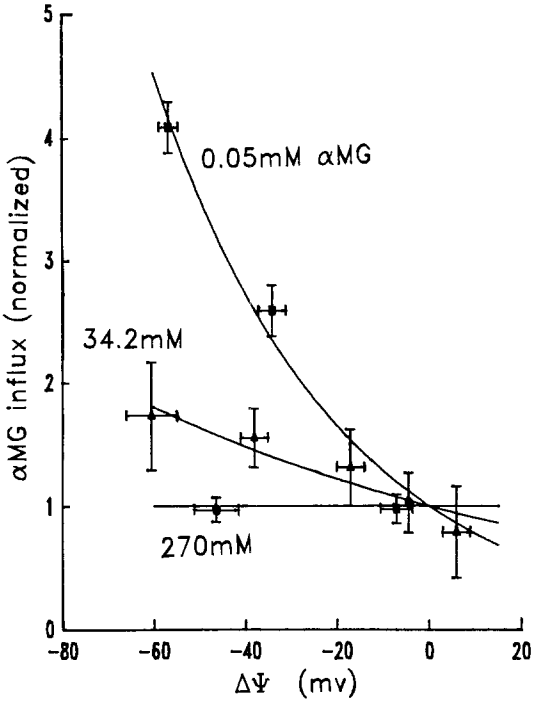

Fig. 5. Normalized α-methylglucoside influx *vs.* membrane potential at 36 mM Na^+. The membrane potential was calculated using the TPP^+ influx technique described in Materials and Methods. Cells were isolated in KG media supplemented by either 0, 38 or 300 mM mannitol. After isolation, they were deenergized by addition of 80 μM rotenone, 200 μM ouabain and 10 μg/ml valinomycin. At the start of the influx, cells were diluted in isosmolar media containing (final amounts) 36 mM Na^+, different amounts of potassium (replaced by TMA^+) and sugar (0.05, 34.2 or 270 mM). The data from each experiment were fit using Eq. (3) and normalized dividing the influx values by the best fit parameter N. The normalization factors are: for 0.05 mM sugar, n = 0.67, N = 0.028 nm μl^{-1} min^{-1} n = 3; for 34.2 mM sugar, n = 0.26, N = 15.21 nm μl^{-1} min^{-1} n = 3; and for 270 mM sugar, n = 0.02, N = 36.85 nm μl^{-1} min^{-1} n = 4

Membrane Potential Dependence of Na^+-Dependent Sugar Influx

Using the TPP^+ influx technique, we have determined the dependence of sugar influx on $\Delta\psi$. Figure 5 shows the dependence at 36 mM sodium (zero-trans) and for three different concentrations of sugar: 0.05 $\ll K_{ms}$, 34.2 mM $> K_{ms}$ and 270 mM $\gg K_{ms}$ (K_{ms}, the Michaelis-Menten constant for sugar influx, is approximately 9 mM at −60 mV). As

Table 1. Results from the best fit of Eq. (3) to the data in Figs. 5 and 6

Sodium (mM)	α-Methylglucose (mM)	N (nm · μl^{-1} · min^{-1} ± SEM)	η^b (± SEM)	n
36	0.05	0.045 ± 0.013	0.62 ± 0.4	6[a]
36	270.0	36.9 ± 3.15	0.02 ± 0.01	4
136	0.05	0.12 ± 0.02	0.61 ± 0.04	4
136	57.0	31.4 ± 4.1	0.10 ± 0.08	5

[a] Three additional experiments are included at 50 μM α-methylglucose and 36 mM sodium.
[b] η is defined by Eq. (3).

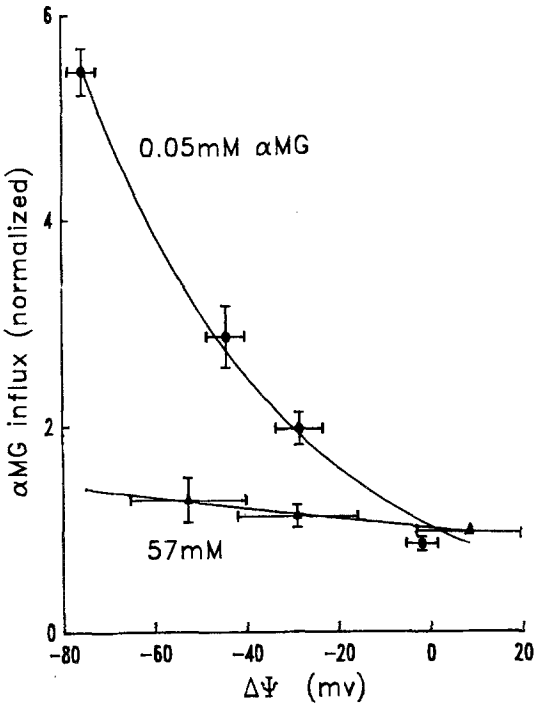

Fig. 6. Normalized α-methylglucoside influx *vs.* membrane potential at 136 mM Na^+. Cells were isolated in a solution containing in mM: 180 K-gluconate, 151 TMA-gluconate, 1 $CaSO_4$, 1 $MgSO_4$ and 25 HEPES-Tris, pH 7.4, at 37°C plus either 0 or 60 mannitol. Cells were de-energized by the addition of 80 μM rotenone, 200 μM ouabain and 40 μg/ml valinomycin. At the start of the influx, cells were diluted in media such that final concentrations were (in addition to the divalent cations and the buffer) in mM: 136 sodium, 195 K^+ plus TMA^+, 195 gluconate plus nitrate, and either 0.05 or 57 mM sugar. The data from each experiment were fit using Eq. (3) and normalized by dividing the influx value by the best-fit parameter N

shown, the degree of potential sensitivity is highly dependent on sugar concentration. In order to quantitate the degree of potential dependence we have fit the experimental data using the equation:

$$\text{FLUX} = N\,\text{EXP}(-\eta\Delta\psi F/RT) \qquad (3)$$

Table 2. Lack of transinhibition of Na^+-dependent sugar influx by sugar[a]

[αMG] (mM)	$\Delta\psi$ (mV)	αMG influx (nm · μl^{-1} · min^{-1})
0.0	−8.75 ± 4	0.487 ± 0.036
40.0	−8.75 ± 4	0.524 ± 0.073
0.0	−109.5 ± 21	4.42 ± 0.46
40.0	−109.5 ± 21	3.91 ± 0.78

[a] The cells were isolated and ATP depleted in a medium containing 150 mM K-gluconate, 100 mM TMA-gluconate, 40 mM mannitol, 1 mM $CaSO_4$, 1 mM $MgSO_4$, 25 mM HEPES-Tris (pH 7.4) and 1 mg/ml BSA. αMG or mannitol were loaded by preincubation of the ATP-depleted cells at 37°C for 40 min. Equilibration of the sugar was verified in parallel incubations with radioactive αMG. Influx was initiated by dilution of the mannitol or αMG-loaded cells 40-fold into a medium containing 150 mM K-gluconate and 100 mM Na-gluconate or into 150 mM $TMANO_3$ and 100 mM $NaNO_3$. The extracellular αMG concentration was 1 mM. Membrane potential was determined using the TPP^+ influx technique by comparison to dilutions in which the preincubation and incubation media were identical. The extracellular sugar concentration was 1.0 mM. Membrane potential was monitored using TPP^+ influx.

where the parameter η provides a relative index of the sensitivity to $\Delta\psi$. As shown in Table 1, this parameter ranges from zero at 270 mM sugar (no dependence on $\Delta\psi$) to 0.62 at 0.05 mM sugar. We have previously shown that the dependence of sugar influx on sugar concentration exhibits a hyperbolic relationship (Restrepo & Kimmich, 1985*a*). In kinetic terms, the results of Fig. 5 can be translated into a large dependence of the Michaelis constant (K_{ms}) on the potential, but no potential dependence for the maximum velocity (J_{ms}).

Because a change in sodium concentration from 36 to 136 mM changed the kinetics of sugar influx significantly (3.6-fold change in K_{ms}; Restrepo & Kimmich, 1985*a*), the effect of changing sodium concentration on potential sensitivity of sugar fluxes was also checked. The data shown in Fig. 6 depicts the membrane potential dependence of sugar influx at 136 mM sodium. As shown in Table 1, the degree of potential dependence (quantitated by η) does not change significantly from that observed at 36 mM sodium.

Lack of Transinhibition of Sodium-Dependent Sugar Influx by Intracellular Sugar

Kessler and Semenza (1983) have used the membrane potential dependence of transinhibition of sugar fluxes by intracellular sugar as a criterion to elucidate the nature of the kinetic mechanism of the transporter. As shown in Table 2, we find no trans-

Table 3. Sugar influx in the nominal absence of sodium: Effects of phlorizin and membrane potential[a]

Isolation medium	Dilution medium	αMG influx (nm · μl^{-1} · min^{-1})	Normalized influx	[Sodium] (μM)	Calculated $\Delta\psi$ (mV)	
KCl	TCl		1.05 ± 0.08	53 ± 70	−52.0	5
KCl	TCl + Pz		1.02 ± 0.18	53 ± 70	−52.0	5
KCl	KCl		0.88 ± 0.14	189 ± 8	0.0	5
KCl	KCl + Na		1.01 ± 0.15	553 ± 70	−52.0	5
KG	TG		0.97 ± 0.14	92 ± 83	−83.0	3
KG	TG + Pz		1.06 ± 0.02	92 ± 83	−83.0	3
KG	KG		0.98 ± 0.15	759 ± 44	0.0	3
KCl	NaCl	2.25 ± 0.71		133 ± mM	−50.0	4
Average of low Na		0.027 ± 0.013				8

[a] Influx of α-methylglucoside (0.5 mM) was measured in cells isolated and de-energized in either KG media (3 expts) or KCl media (5 expts) (5 to 16% vol/vol of cells) and diluted 20-fold into different solutions in the nominal absence of sodium. Cells were preincubated for 15 min at 37°C and washed twice (0.3 to 1% vol/vol cells). All solutions contained 40 μg/ml valinomycin. In some cases, 1.33 mM phlorizin (+Pz) or 500 μM sodium (+Na) (final concentrations) were added to the extracellular solution. Rates were normalized to the average rate from each experiment. Sodium concentrations were measured by flame photometry. The membrane potentials were calculated using relative ion permeabilities measured using the crossover technique (Kimmich et al., 1985*a*). (All values are shown ± SD.)

inhibition by sugar under conditions similar to those used by Kessler and Semenza (1983) for rabbit intestine. A 100-mV change in the membrane potential does not unmask transinhibition by sugar.

Sugar Fluxes in the Nominal Absence of Sodium

Sugar fluxes in the absence of sodium are independent of the membrane potential and are not inhibited by high concentrations (1.33 mM) of phlorizin, an inhibitor of sodium-dependent sugar transport (Table 3). Extracellular sodium for these experiments was measured by flame photometry and is shown in the table. The rates shown represent approximately 1.2% of the sugar flux observed in the presence of 133 mM extracellular sodium at a membrane potential of −50 mV. Addition of 500 mM extracellular sodium does not change the sugar influx rate ruling out involvement of the sodium-dependent system. This agrees with calculations using the Hill parameters found for sodium-dependent sugar transport in Restrepo and Kimmich (1985*a*) which predict that sodium-dependent sugar influx is negligible at 500 μM sodium (0.004% of the rate at 133 mM sodium).

Dependence of Phlorizin Inhibition Kinetics on the Membrane Potential

Various studies on phlorizin binding have indicated that binding is a potential-sensitive event (Tannen-

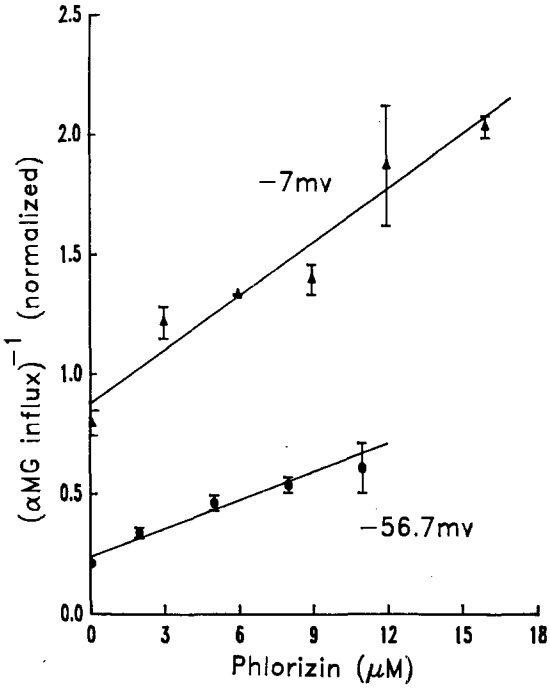

Fig. 7. Changes in the membrane potential modify the ID_{50} for phlorizin inhibition of sugar transport at low sugar concentrations (0.05 mM). Cells were isolated in KG media and were de-energized by addition of rotenone, ouabain and 10 μg/ml of valinomycin. At the start of the influx, a cell aliquot was diluted into media containing either 14 or 104 mM potassium (replaced by TMA^+) and 36 mM sodium (all gluconate salts). In addition, 0.05 mM sugar and different amounts of phlorizin were present. The data were normalized by dividing by a number such that the uninhibited flux at −56.7 mV was 4.2 which is the value of the point at −56.7 mV in Fig. 5

baum et al., 1977; Aronson, 1978; Toggenburger et al., 1978, 1982; Turner & Silverman, 1981). Figure 7 shows that there is also a change in the extent of inhibition of sugar fluxes by phlorizin in our system when the membrane potential is changed. In this set of experiments, the ID_{50} for phlorizin decreases from 12.4 ± 1.2 μM at −7 mV to 6.2 ± 0.6 μM at −56.7 mV (avg ± SD, n = 3).

Discussion

Although sodium-dependent sugar transport was shown to be enhanced by inside-negative membrane potentials a decade ago by Murer and Hopfer (1974), our understanding of the mechanistic significance of the potential dependence is still limited. The experimental results presented from other laboratories which are most directly relevant to the elucidation of potential dependence including the following:

1. Tannenbaum et al. (1977), Toggenburger et al. (1978), Aronson (1978), Turner and Silverman (1981), and Toggenburger et al. (1982) have shown that the association rate for phlorizin in the presence of sodium is enhanced by inside-negative membrane potentials, and that the dissociation rate is potential-insensitive. These investigators also found that the association rate constant is increased and that the dissociation rate constant is decreased by extracellular sodium.

2. Kessler and Semenza (1983) reported that transinhibition of sugar influx by sugar is relieved by inside-negative membrane potentials.

3. Hilden and Sacktor (1982) have shown that in the kidney a portion of the influx of D-glucose in the nominal absence of sodium is membrane potential dependent and is inhibited by phlorizin. The binding of phlorizin in the absence of sodium was also found to be potential dependent. In addition, sugar specificity and stereospecificity in the absence of sodium suggest that under these conditions sugar flux was still mediated by the sodium-dependent transporter for their experimental system.

Kessler and Semenza (1983) have proposed a model for sodium-dependent sugar transport in intestine which provides a mechanistic basis for explaining the various properties mentioned above. The proposed model involves transport via an asymmetric gated pore which behaves kinetically like a carrier for which translocation across the membrane is potential dependent. In order to explain the membrane potential dependence of phlorizin binding and the relief of transinhibition by inside-negative membrane potentials they postulate that the free carrier is negatively charged. For this model, transduction of electrical energy into chemical energy occurs due to a potential-dependent redistribution of carrier between cytoplasmic and extracellular membrane interfaces.

However, transduction of electrical energy to chemical energy does not have to occur during the translocation step: it could also occur at the sodium binding step if the binding site is located within the membrane in a manner analogous to the proton well proposed by Mitchell to explain the transduction of energy in the proton ATPase (Mitchell, 1969; Maloney, 1982). This idea was proposed by Hopfer and Groseclose (1980) as a possible mechanism for the sodium-sugar cotransporter and was evaluated for the kidney sodium-sugar cotransporter in an article by Aronson (1984).

Aronson explains that (for a 1 phlorizin to 1 sodium model) if sodium inhibits dissociation and if sodium binding to its site is potential dependent, then phlorizin debinding should be potential dependent (which is not). This paradox is a valid reason to discard a sodium well model if the stoichiometry were 1 sodium to 1 phlorizin. However, the only evidence for a 1 : 1 phlorizin/sodium stoichiometry comes from Hill plots for phlorizin bound *vs.* sodium concentration (Aronson, 1978; Turner & Silverman, 1981; Toggenburger et al., 1982). In an earlier paper, we have analyzed the limitations of drawing conclusions about coupling stoichiometry strictly from kinetic data (Restrepo & Kimmich, 1985*a*). These limitations, compounded by the fact that in at least one report the plot of phlorizin bound *vs.* phlorizin bound divided by sodium concentration is nonlinear (Turner & Silverman, 1981), lead us to believe that it is premature to discard the sodium well idea based on an assumed 1 : 1 sodium/phlorizin stoichiometry.

If 2 sodium : 1 phlorizin models are considered, it is not difficult to explain the phlorizin data. For instance, consider a model in which the first sodium has to traverse a fraction of the electric field in order to reach its binding site, but the second sodium binding site is located near the outer face of the membrane. In this model, membrane potential dependence for the rate of phlorizin association and the ID_{50} for phlorizin inhibition (Fig. 7) are due to the strong potential dependence of the binding of the first sodium. Conversely, the potential independence of the dissociation rate constant for phlorizin is due to the weak potential dependence of the binding of the second sodium. In addition, the inhibition of phlorizin debinding by external sodium is explained by the binding of the second sodium which could trap phlorizin in the ternary complex (2 sodium : 1 phlorizin).

Hilden and Sacktor's (1982) observation that

sugar fluxes depend on the membrane potential in the nominal absence of sodium could be used to rule out a sodium well type of mechanism. However, this phenomenon was reported for rabbit kidney, and does not occur in chick intestine. In fact, for isolated chick intestinal cells, the data in Table 3 show that sugar fluxes in the absence of sodium are neither inhibited by large amounts of phlorizin (1.33 mM) nor influenced by the membrane potential. The magnitude and characteristics of the sugar fluxes observed in the absence of sodium are inconsistent with them being related to function of the Na^+-dependent carrier. They probably represent diffusional fluxes via a completely independent route for the chick epithelial system. The observations of Hilden and Sacktor (1982) cannot be used as the only reason to rule out a kinetic model involving potential-dependent Na^+ binding without further corroboration and supporting evidence.

The data presented in Figs. 5 and 6 place additional restrictions on acceptable kinetic models for the sodium-sugar cotransporter. A satisfactory model must predict the observed high degree of potential dependence for the Michaelis constant for sugar (K_{ms}) and the low degree of potential dependence for the maximum velocity for sugar influx (J_{ms}). In order to evaluate the mechanistic implications of this change in the degree of potential dependence, we have used Eyring formalism (Eyring et al., 1949) to introduce the membrane potential dependence in the flux equation for the terter model with binding order sodium/sugar/sodium (N/S/N). This model, shown in Fig. 8, was chosen based on earlier kinetic studies which identify it as a likely choice for sodium-sugar cotransport (Kimmich & Randles, 1984; Restrepo & Kimmich, 1985*a*). The models considered were: 1) those for which translocation is the membrane potential-dependent step with the free carrier bearing a charge of either zero (neutral carrier model) or -1 or -2 (anionic free carrier model); and 2) a model for which binding of sodium is the membrane potential-dependent step (sodium well model).

The flux equations were derived using the King-Altman procedure (Restrepo & Kimmich, 1985*a*), assuming either that translocations of the carrier across the membrane are the rate-limiting steps, or with no assumption regarding a rate-limiting step. The rate-limiting step assumption simplifies the form of the equation considerably (*see* Appendix for derivations). It is not known whether translocation is rate limiting for sodium-sugar cotransport (Restrepo & Kimmich, 1985*a*), and hence ruling out models derived under this assumption is important for further elucidation of the transport mechanism. Without this assumption, the flux equation is very

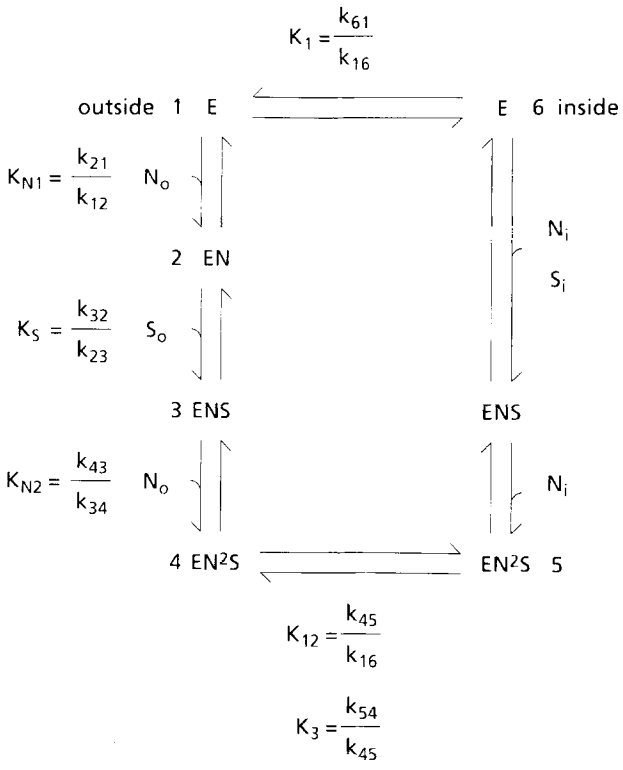

Fig. 8. Terter model with binding order sodium/sugar/sodium (NSN). This model provides a mechanistic basis for the observed membrane potential behavior of sugar fluxes

complex (the equation has from 13 to 16 independent parameters depending on the form of membrane potential dependence). We have used numerical methods to fit equations derived without rate-limiting step assumptions to the experimental data in order to identify specific models which can be excluded.

Using the rate-limiting step assumption, it can be shown that, in order for the negatively charged free carrier model to fit the membrane potential dependence determined in Figs. 5 and 6, the amount of free carrier facing the extracellular interface at zero membrane potential must be less than $\frac{1}{3}$ the amount of free carrier at the cytoplasmic interface (*see* Appendix). Table 4 is a compilation of computer fits of several transport parameters for various transport models in comparison to experimentally observed values for these parameters. Computer calculated binding constants and other relevant transport constants are given for each model. The data show that even when the rate-limiting step assumption is relaxed, the best fits of models with anionic free carriers all yield $K_1 < 1$ indicating an asymmetric distribution of free carrier. This functional asymmetry is expected for these models

Table 4. Nonlinear least-squares fit results

Model	Fit criteria							Parameters					
	η^d	η^e	η^f	η^g	J_{ms} ratio[h]	K_{ms} ratio[i]	Sum of square residues	δ_1	δ_2	K_1	K_{12}	K_{N1} (mM)	K_{N2} (mM)
Experimental values	0.62 ± 0.04	0.61 ± 0.04	0.02 ± 0.1	0.1 ± 0.08	1.5 ± 0.1	0.28 ± 0.04							
NC[a]	0.62	0.61	0.033	0.017			1.19	0.31		0.039	2.38	6.22	176.2
NC[b]	0.59	0.59	0.34	0.22	1.41	0.28	15.6	0.30		1.87	8.83	22.7	379
NC[c]	0.67	0.55	0.09	0.10	1.52	0.14	14.1	0.60		0.11	0.78	155.9	97.96
IC[b]	0.71	0.54	0.06	0.08	1.53	0.15	15.9	0.79	0.02	0.08	0.56	210.5	56.36
IC[c]	0.69	0.55	0.07	0.13	1.51	0.28	5.6	0.43	0.42	0.08	0.001	344	2.710^{-4}
2C[b]	0.72	0.54	0.08	0.15	1.53	0.32	18.4	0.79		0.09	0.09	890	58
2C[c]	0.70	0.47	0.08	0.13	1.51	0.23	17.9	0.68		0.10	2.14	861	147.5
NW[b]	0.64	0.50	0.23	0.12	1.49	0.28	12.7	0.43	0.41	2.72	1.33	57.8	100.3
NW[c]	0.62	0.61	0.01	0.005	1.48	0.30	1.9	0.62	0.03	0.002	0.004	71.6	92.5

This table shows the results of computer fits of the experimental data on membrane potential and sodium dependence of the maximum velocity (J_{ms}) and the Michaelis constant (K_{ms}) for sugar transport by different kinetic models. The membrane potential criteria used in the fit are the experimentally determined values for η displayed in Table 4. The sodium dependence criteria are values of the ratio (at $\Delta = -43$ mV) of the value for J_{ms} or K_{ms} at 136 mM sodium to the value of the same parameter at 40 mM sodium (from Restrepo & Kimmich, 1985*a*). The detailed procedure of the fit is described in the Appendix. The sodium binding constants K_{N1}, K_{N2}, the free carrier asymmetry constant K_1 and K_2 are defined in terms of rate constants in Fig. 8. All values shown for these constants are at $\Delta = 0$. δ_1 and δ_2 are constants whose values range from zero to one as defined in the Appendix and relate to the shape or location of the free energy barrier of the membrane potential-dependent steps of the different kinetic models. The models used are: neutral carrier model (NC), anionic free carrier models with charge −1 (1C) or −2 (2C) and sodium well model (NW).

[a] Fit of the membrane potential dependence data alone.

[b] Fit of model assuming translocation is rate limiting.

[c] Fit assuming no rate-limiting step.

[d] At 50 μM sugar and 36 mM Na^+.

[e] At 50 μM sugar and 136 mM Na^+.

[f] At 270 mM sugar and 36 mM Na^+.

[g] At 57 mM sugar and 136 mM Na^+.

[h] J_{ms} ratio 136 mM Na^+ to 40 mM Na^+.

[i] K_{ms} ratio 136 mM Na^+ to 40 mM Na^+.

on physical grounds alone because for anionic free carrier models, transduction of electrical energy into chemical energy takes place by redistribution of the carrier. In fact, the models predict that if there is more free carrier at the extracellular side than at the cytoplasmic side when the membrane potential is zero, then the potential dependence of sugar fluxes will be greatly reduced. This observation is consistent with conclusions by Kessler and Semenza (1983) on functional asymmetry of anionic carrier models.

The potential independence of the maximum velocity (J_{ms}) and the dependence of the Michaelis constant (K_{ms}) can be modeled by the neutral carrier model if translocation of the free carrier is slower than translocation of the loaded carrier (under the assumption that translocation is rate limiting; *see* Appendix for derivations and Table 4 for an example of a fit of the model to the potential behavior). However, under these conditions the model displays no dependence of the maximum velocity J_{ms} on sodium concentration. The model predicts that the ratio of maximum velocities at 136 *vs.* 40 mM sodium is 1 in contradiction with our results reported earlier which yield a ratio of 1.5 ± 0.1 (avg ± SD) for these sodium concentrations (Restrepo & Kimmich, 1985*a*).[2] This agrees with Kessler and Semenza's (1983) conclusion that the model where the free carrier bears no charge can be discarded although they base this conclusion on relief of trans-inhibition by interior negative membrane potentials.

As mentioned before, in Restrepo and Kimmich (1985*a*) we found that the terter NSN model is the simplest model to fit the sodium and sugar dependence of sugar fluxes. However, in the same paper we mention that the random order 2 sodium : 1 sugar model could also fit the data. In the Appendix

[2] In Restrepo and Kimmich (1985*a*), this ratio was calculated using a normalization procedure to correlate data from different experiments. We have confirmed these results by direct measurements of sugar influx at 270 mM sugar $\Delta\psi = -50$ mV. Results of these experiments yield 1.59 ± 0.09 (mean ± SE, n = 3) for the ratio of maximum velocities at 136 *vs.* 40 mM sodium.

we show that, as in the case of the terter NSN model, the maximum velocity for sugar transport predicted by this model under the translocation rate-limiting step assumption can be set constant as a function of the membrane potential. However, under these conditions, the maximum velocity is not dependent on sodium concentration contrary to data in Restrepo and Kimmich (1985*a*). Hence, the neutral free carrier model can also be discarded for the random order scheme.

It is important to point out that the theoretical derivation in the Appendix as well as in Kessler and Semenza's (1983) paper of the equations which allow discarding the neutral carrier model both carry the assumption that translocation is rate limiting The neutral carrier model can also be discarded on other grounds. As stated by Aronson (1984), in order to explain the membrane potential dependence of phlorizin binding, one must postulate that the sodium/phlorizin-loaded carrier is translocated across the membrane. However, in this case, the debinding of phlorizin would be potential dependent contrary to their experimental observations. Thus, the neutral carrier model can be discarded on the basis of observations on the potential dependence of phlorizin binding, sugar transinhibition, and the criteria used in Table 4.

In the present report, no transinhibition by sodium or sugar was found under conditions similar to those used by Kessler and Semenza (1983). It is important to state that this discrepancy does not necessarily mean that the kinetic mechanisms themselves are different for the two preparations. For any kinetic model, transinhibition effects tend to be smaller if translocation events are slow compared to binding and debinding of the transported species at the trans side. Hence, a difference in the kinetic constants, due to inherent differences in membrane carrier properties between rabbit and chicken, might modify the transinhibition response. A difference in intracellular sugar binding affinities could also account for the difference in transinhibition. In fact, comparison of the K_{ms} for D-glucose in Kessler and Semenza's (1983) study (0.7 mM at $\Delta\psi = 0$ and $Na^+ = 120$ mM) with the K_{ms} in chicken cells (11 mM at $\Delta\psi = 0$ and $Na^+ = 136$ mM)[3] suggests that the intracellular binding affinity for sugar could differ in the two experimental systems.

The sodium well model can fit the membrane potential-dependence criteria and the sodium-dependence criteria reasonably well when translocation is assumed to be the rate-limiting step (Table 4). However, if this assumption is relaxed and it is assumed that the sugar binding step is not at equilibrium, the sodium well model displays the best fit of all models tested. In addition, the sodium well mechanism can model the relief of transinhibition by inside-negative membrane potentials (Kessler & Semenza, 1983). For instance, if the binding order at the trans side is sodium/sugar/sodium, the relief of transinhibition could be due to the enhancement of the debinding of the second sodium by inside-negative membrane potentials leading to a shorter half-life of the inward-facing sodium-loaded carrier which is the carrier form that binds intracellular sugar.

Thus, with the data currently available for the intestinal sodium-dependent sugar transporter, it is not possible to distinguish between a sodium well model and a model in which translocation of the carrier (either loaded or unloaded) is the membrane potential-dependent step. However, the cumulative information available allows further constraining of each class of model. For example, the sodium well model cannot explain the data on the membrane potential dependence of phlorizin if the sodium/phlorizin stoichiometry is shown to be 1 : 1. On the other hand, from our observations on the potential dependence of sugar fluxes and observations from other laboratories on the potential dependence of transinhibition, and phlorizin binding, it can be concluded that if translocation is the potential-dependent step, then the free carrier must bear a net charge and the free carrier must be distributed asymmetrically across the membrane at zero membrane potential. The ordered terter model with binding order sodium/sugar/sodium (NSN) (Fig. 8) can be used successfully to describe the sodium and sugar dependence of sugar fluxes at a fixed membrane potential (Restrepo & Kimmich, 1985*a*) and is shown in this report to be able to provide a mechanistic basis for our observations on the membrane potential dependence of sugar fluxes, of phlorizin inhibition, and to the observations of other investigators on the membrane potential dependence of phlorizin binding (Tannenbaum et al., 1977; Aronson, 1978; Toggenburger et al., 1978, 1982; Turner & Silverman, 1981) and transinhibition of sugar fluxes (Kessler & Semenza, 1983).

[3] The K_{ms} for sugar transport in chicken cells at $\Delta\psi = 0$ and $Na^+ = 136$ mM was calculated using the measured value of the K_{ms} at $\Delta\psi = -43$ mV and $Na^+ = 136$ mM (from Restrepo & Kimmich, 1985*a*) and the calculated value for η at 136 mM sodium and 0.05 mM sugar shown in Table 3.

We acknowledge the excellent technical assistance provided by Mrs. Geraldine Bebernitz, the fruitful discussions and support of Dr. Philip Knauf and the help of Dr. William P. Cacheris who provided us with a BASIC version of the simplex algorithm. This work was supported by the National Institute of Arthritis, Metabolism and Digestive Diseases Grant AM-15365.

References

Aronson, P.S. 1978. Energy-dependence of phlorizin binding to isolated renal microvillus membranes. *J. Membrane Biol.* **42:**81–98

Aronson, P.S. 1984. Electrochemical driving forces for secondary active transport: Energetics and kinetics of Na^+-H^+ exchange and Na^+-glucose cotransport. *In:* Electrogenic Transport: Fundamental Principles and Physiological Implications. M.P. Blaustein and M. Liberman, editors. pp. Raven, New York

Caceci, M.S., Cacheris, W.P. 1984. Fitting curves to data. The simplex algorithm is the answer. *Byte* **May issue:**340–362

Carter-Su, C., Kimmich, G.A. 1979. Membrane potentials and sugar transport by ATP-depleted intestinal cells: Effect of anion gradients. *Am. J. Physiol.* **6:**C67–C74

Eyring, H., Lumry, R., Woodbury, J.W. 1949. Some applications of modern rate theory to physiological systems. *Rec. Chem. Prog.* **10:**100–114

Goldman, D.E. 1943. Potential, impedance, and rectification in membranes. *J. Gen. Physiol.* 27–60

Gornall, A., Bardawill, C., David, M. 1979. Determination of serum protein by means of the biuret reaction. *J. Biol. Chem.* **177:**751–758

Gunther, R.D., Schell, R.E., Wright, E.M. 1984. Ion permeability of rabbit intestinal brush border membrane vesicles. *J. Membrane Biol.* **78:**119–127

Hilden, H., Sacktor, B. 1982. Potential-dependent D-glucose uptake by renal brush border membrane vesicles in the absence of sodium. *Am. J. Physiol.* **242:**F340–F345

Hopfer, U., Groseclose, R. 1980. The mechanism of Na^+-dependent D-glucose transport. *J. Biol. Chem.* **255:**4453–4462

Kanuitz, J.D., Wright, E.M. 1984. Kinetics of sodium D-glucose cotransport in bovine intestinal brush border vesicles. *J. Membrane Biol.* **79:**41–51

Kessler, M., Semenza, G. 1983. The small intestinal Na^+, D-glucose cotransporter: An asymmetric gated channel (or pore) responsive to $\Delta\psi$. *J. Membrane Biol.* **76:**27–56

Kimmich, G.A. 1970. Preparation and properties of mucosal epithelial cells isolated from small intestine of the chicken. *Biochemistry* **9:**3659–3668

Kimmich, G.A., Randles, J. 1984. Sodium-sugar coupling stoichiometry in chick intestinal cells. *Am. J. Physiol.* **247:**C74–C82

Kimmich, G.A., Randles, J., Restrepo, D., Montrose, M. 1985*a*. A new method for determination of relative ion permeabilities in isolated cells. *Am. J. Physiol. (in press)*

Kimmich, G.A., Randles, J., Restrepo, D., Montrose, M. 1985*b*. The potential dependence of the intestinal Na^+-dependent sugar transporter. *Ann. N.Y. Acad. Sci. (in press)*

Maloney, P.C. 1982. Energy coupling to ATP synthesis by the proton-translocating ATPase. *J. Membrane Biol.* **67:**1–12

Mitchell, P. 1969. Chemiosmotic coupling and energy transduction. *Theor. Exp. Biophys.* **2:**159–216

Murer, M., Hopfer, U. 1974. Demonstration of electrogenic Na^+-dependent D-glucose transport in intestinal brush border membranes. *Proc. Natl. Acad. Sci. USA* **71:**484–488

Picone, A. 1977. Characteristics of amino acid transport in the isolated small intestinal epithelial cell. Doctoral dissertation. Department of Radiation Biology and Biophysics, University of Rochester, Rochester, N.Y.

Restrepo, D., Kimmich, G.A. 1985*a*. Kinetic analysis of the mechanism of intestinal Na^+-dependent sugar transport. *Am. J. Physiol. (in press)*

Restrepo, D., Kimmich, G.A. 1985*b*. Electrical potential dependence of Na^+-sugar co-transport determined using TPP^+ influx. *Ann. N.Y. Acad. Sci. (Abstr.) (in press)*

Rose, R.C., Schultz, S.G. 1971. Studies on the electrical potential profile across rabbit ileum: Effects of sugars and amino acids on transmural and transmucosal electrical potential differences. *J. Gen. Physiol* **57:**639–663

Schell, R.E., Stevens, B.R., Wright, E.M. 1983. Kinetics of sodium-dependent solute transport by rabbit jejunal brush-border vesicles using a fluorescent dye. *J. Physiol. (London)* **335:**307–318

Semenza, G., Kessler, M., Hosang, M., Weber, J., Schmidt, U. 1984. Biochemistry of the Na^+, D-glucose cotransporter of the small intestinal brush border membrane. The state of the art in 1984. *Biochim. Biophys. Acta* **779:**343–379

Semenza, G., Kessler, M., Schmidt, U., Venter, C., Fraser, C. 1985. The small-intestinal sodium-glucose cotransporter(s). *Ann. N.Y. Acad. Sci. (in press)*

Squires, G.L. 1976. Practical Physics. McGraw-Hill, London

Tannenbaum, C., Toggenburger, G., Kessler, M., Rothstein, A., Semenza, G. 1977. High-affinity phlorizin binding to brush border membranes from small intestine: Identity with (a part of) the glucose transport system, dependence on the Na^+ gradient, partial purification. *J. Supramol. Struct.* **6:**519

Toggenburger, G., Kessler, M., Rothstein, A., Semenza, G., Tannenbaum, C. 1978. Similarity in effects of Na^+ gradients and membrane potentials on D-glucose transport by, and phlorizin binding to, vesicles derived from brush borders of rabbit intestinal mucosal cells. *J. Membrane Biol.* **40:**269–290

Toggenburger, G., Kessler, M., Semenza, G. 1982. Phlorizin as a probe of the small intestinal Na^+, D-glucose cotransporter. A model. *Biochim. Biophys. Acta* **688:**557–571

Turner, R.J., Silverman, M. 1981. Interaction of phlorizin and sodium with the renal brush-border membrane D-glucose transporter: Stoichiometry and order of binding. *J. Membrane Biol.* **58:**43–55

White, J. F., Armstrong, W. McD. 1971. Effect of transported solutes on membrane potentials in bullfrog small intestine. *Am. J. Physiol.* **221:**914–201

Received 26 March 1985; revised 10 June 1985

Appendix

Membrane Potential Dependence of the Ordered Terter NSN Model and Partial Analysis of the Random Order 2 Sodium : 1 Sugar Model

Flux Equation Assuming that Translocation is Rate Limiting

In a previous paper on sugar kinetics, we derived the equation for the flux of sugar (J) *vs.* sugar (S) and sodium (N) concentrations for the ordered terter model with binding order NSN under the assumption that translocation steps are rate limiting (Restrepo & Kimmich, 1985*a*). This terter model is depicted in Fig. 8 and the flux equation is given below.

$$\frac{J}{\rho} = k_{45}K_1N^2S/((K_{12} + K_1)N^2S + K_1K_{N2}NS + K_1K_SK_{N2}N + (K_1 + 1)K_{N1}K_{N2}K_S). \quad \text{(A1)}$$

The definition of the parameters is shown in Fig. 8. N and S are sodium and sugar concentration, respectively, and ρ is a factor that changes depending on the units for flux (J).

The maximum velocity J_{ms} and the Michaelis-Menten constant K_{ms} for the dependence of the sugar flux as a function of sugar concentration and the ratio J_{ms}/K_{ms} are shown below.

$$J_{ms} = \rho k_{45}N/(K_{N2} + (1 + K_{12}/K_1)N) \quad \text{(A2)}$$

$$K_{ms} = K_SK_{N2}(N + (1 + (1/K_1))K_{N1})/N(K_{N2} + (1 + (K_{12}/K_1))N) \quad \text{(A3)}$$

$$J_{ms}/K_{ms} = \rho k_{45}N^2/K_SK_{N2}(N + (1 + (1/K_1))K_{N1}). \quad \text{(A4)}$$

Flux Equation with no Rate-Limiting Step

If no rate-limiting step is assumed, the flux equation for sugar as a function of sugar and sodium concentrations can be expressed in the form:

$$J = J_{ms}S/(K_{ms} + S) \quad \text{(A5)}$$

where:

$$J_{ms} = \rho k_{45}K_1N^2/\Sigma \quad \text{(A6)}$$

$$K_{ms} = K_S[K_{N2}(K_1N + K_{N1}(K_1 + 1)) + \frac{k_{45}}{k_{34}}(K_1(N + K_{N1}) + K_{N1}) + \frac{k_{45}}{k_{56}}K_3(K_1(K_{N2}N + K_{N1}K_{N2}) + K_{N1}K_{N2}) + \frac{k_{45}}{k_{23}}(K_1(N^2 + NK_{N1}) + K_{N1}N)]/\Sigma \quad \text{(A7)}$$

$$\Sigma = (K_{12} + K_1)N^2 + K_1K_{N2}N + \frac{k_{45}}{k_{56}}(N^2K_1(1 + K_3) + K_1K_3K_{N2}N) + \frac{k_{45}}{k_{34}}K_1N + \frac{k_{45}}{k_{12}}(N(1 + K_1)). \quad \text{(A8)}$$

These equations reduce to the translocation rate-limiting case if the parameters $\frac{k_{45}}{k_{23}}$, $\frac{k_{45}}{k_{34}}$, $\frac{k_{45}}{k_{12}}$, and $\frac{k_{45}}{k_{56}}$ are set equal to zero.

Membrane Potential Dependence

To model the membrane potential dependence, it was assumed that the rate constants for the potential-dependent steps of the mechanism depend on $\Delta\psi$ as proposed by Eyring et al. (1949) and given by Eq. (A9).

$$k_\pm = k_{\pm 0}e^{-\delta z\Delta\psi F/RT} \quad \text{(A9)}$$

where $k_\pm$ are forward or backward rate constants, z is the charge of the potential-dependent species, and δ is the fraction of the electric field that the charged particle has to traverse in order to reach the highest point of the energy barrier in a free-energy diagram.

Models in which Translocation is the Potential-Dependent Step

A. Ruling out the translocation model where the free carrier is neutral.

For this model, the potential-dependent parameters are:

$$k_{45} = k_{450}e^{-2\delta_1 x};\ K_{12} = K_{120}e^{-2\delta_1 x} \quad \text{(A10)}$$

where k_{450} and k_{120} are independent of the membrane potential and $x = \Delta\psi F/RT$.

The ratio J_{ms}/K_{ms} depends on the membrane potential as a function of $\exp(-2\delta_1 x)$. Comparing this with Eq. (3) which fits the data at low sugar, we can equate δ_1 to $(n/2) = 0.31$. Since we found that the maximum velocity J_{ms} does not depend on the membrane potential (Figs. 5 and 6), this means that the following equation holds true:

$$[K_{ms}(x_1)/K_{ms}(x_2)] = e^{-2\delta_1(x_2 - x_1)}. \quad \text{(A11)}$$

But since from Eq. (A3) we can derive:

$$[K_{ms}(x_1)/K_{ms}(x_2)] = \frac{y + e^{-2\delta_1 x_2}}{y + e^{-2\delta_1 x_1}} \quad \text{(A12)}$$

where $y = ((K_{N2}/N) + 1)(K_1/K_{120})$, it follows by comparing Eqs. (A11) and (A12) that the factor y is small compared to 1. Using this fact, the ratio of maximum velocities at two different sodium concentrations can be reduced to:

$$[J_{ms}(N_1)/J_{ms}(N_2)] = 1. \quad \text{(A13)}$$

Data from Restrepo and Kimmich (1985*a*) gives 1.5 ± 0.1 for the ratio of maximum velocities $[J_{ms}(136)/J_{ms}(40)]$ in contradiction with Eq. (A13).

B. The potential-dependent parameters for the mechanism in which the free carrier bears one negative charge are:

$$K_1 = K_{10}e^{-x};\ K_{12} = K_{120}e^{-(\delta_1+\delta_2)x}$$
$$k_{45} = k_{450}e^{-\delta_1 x}. \tag{A14}$$

These expressions were used in the nonlinear least-squares fit described at the end of the Appendix.

C. The translocation model in which the free carrier carries two negative charges must be assymetric to fit the observed potential dependence as shown below.

The potential-dependent parameters in this model are

$$K_1 = K_{10}e^{-2x};\ K_{12} = K_{120}e^{-2\delta_1 x}. \tag{A15}$$

The ratio of J_{ms}/K_{ms} at two membrane potentials is given by

$$\frac{[(J_{ms}/K_{ms}) \text{ at } x_1]}{[(J_{ms}/K_{ms}) \text{ at } x_2]} = \frac{Z + e^{2x_2}}{Z + e^{2x_1}} \tag{A16}$$

where Z is given by

$$Z = K_{10}\left(\frac{N}{K_{N1}} + 1\right). \tag{A17}$$

From the data in Figs. 5 and 6 we can see that this ratio is larger than 4 when the membrane potential is changed from 0 to −60 mV. Hence, $Z < 0.32$. It follows that $K_{10} < 0.32$. Since K_{10} denotes the free carrier distribution at zero potential, it follows that at zero potential there are at least three times as many carriers at the cytoplasmic side of the membrane as at the extracellular side of the membrane. Hence, the kinetic mechanism must be asymmetric in order to fit the dependence shown in Figs. 5 and 6.

Sodium Well Model

For this model, the sodium binding constants depend on the membrane potential as follows:

$$K_{N1} = K_{N10}e^{\delta_1 x}$$
$$K_{N2} = K_{N20}e^{\delta_2 x}. \tag{A18}$$

In these equations, x is $\Delta\psi F/RT$ and δ_1 and δ_2 are the fraction of the electric field drop that each sodium must traverse to get to its binding site.

Nonlinear Least-Squares Fit

To perform the nonlinear least-squares fit, we used the same FORTRAN program used earlier for analyzing the sodium and sugar concentration dependence of sugar transport (Restrepo & Kimmich, 1985*a*) and a BASIC version of the simplex algorithm (Caceci & Cacheris, 1984). The least squares were weighted by a quantity equal to one over the square of the standard error of the mean of the value of each fit criterium (Squires, 1976). The six criteria used for the fit were:

1. The parameter η (defined in Eq. 3) at 36 mM sodium and 270 mM sugar. For these conditions, $\eta = 0.02 \pm 0.1$ and the weight used was 100. η was calculated by using Eq. (A19) which can be derived directly from Eq. (3). The two membrane potentials were −45 and −5 mV. J_{ms} was used instead of J in Eq. (A19) since at this sugar concentration $J = J_{ms}$.

$$\eta = (1/(x_2 - x_1))\ \ln(J(x_1)/J(x_2)). \tag{A19}$$

2. η at 136 mM sodium and 57 mM sugar. $\eta = 0.10 \pm 0.08$; weight = 156. Evaluated as in 1 except that the membrane potentials were 10 and −40 mV.

3. η at 36 mM sodium and 50 μM sugar. $\eta = 0.62 \pm 0.04$; weight = 625. Same as above except J_{ms}/K_{ms} was used instead of J and the membrane potentials used to evaluate Eq. (A19) were −20 and −60 mV.

4. η at 136 mM sodium and 50 μM sugar. $\eta = 0.61 \pm 0.04$; weight = 625. Same as in 3 except that the potentials were −20 and −80 mV.

5. The ratio J_{ms}(136 mM Na)/J_{ms}(40 mM Na) at −43 mV. From Restrepo and Kimmich (1985*a*) this is 1.50 ± 0.060; weight = 278.

6. The ratio K_{ms}(136 mM Na)/K_{ms}(40 mM Na) at −43 mV. From Restrepo and Kimmich (1985*a*) this ratio is 0.276 ± 0.044; weight = 517.

The membrane potential for the last two criteria was calculated from measurements of relative ion permeabilities (Kimmich et al., 1985*a*).

Partial Analysis of the Membrane Potential Dependence of Sugar Influx for the Random Order 2 Sodium : 1 Sugar Model when Translocation is the $\Delta\psi$-Dependent Step and the Free Carrier is not Charged

In Restrepo and Kimmich (1985*a*) we solved the velocity equations for this model under the translocation rate-limiting step assumption. The maximum velocity for sugar transport as a function of sugar is given by Eq. (A20), the sugar flux at low sugar by Eq. (A21) and the membrane potential-dependent constants when translocation is the dependent step and the free carrier is uncharged are given by Eq. (A22).

$$J_{ms} = \rho k_{67}N^2/(K_{N4}K_{N2} + N^2(1 + K_{12}/K_1)) \tag{A20}$$
$$J_x(S \ll K_{ms}) = k_{67}\gamma \tag{A21}$$
$$k_{67} = k_{670}e^{-2\delta_1 x};\ K_{12} = K_{120}e^{-2\delta_1 x}. \tag{A22}$$

The constants used in this equation are defined in Fig. 8 of Restrepo and Kimmich (1985*a*). γ is a constant independent of the membrane potential for the uncharged free carrier model.

In order for J_s to be membrane potential independent, N^2K_{120}/K_{12} must be large. However, in this condition J_{ms} becomes equal to:

$$J_{ms} = \frac{\rho k_{670}K_1}{K_{120}}, \tag{A23}$$

which is sodium independent in contradiction with evidence from Restrepo and Kimmich (1985*a*).